Assessment of Radiometric Accuracy of Landsat-4 and Landsat-5 Thematic Mapper Data Products from Canadian Production Systems

Jennifer M. Murphy, Francis J. Ahern, and *Paul F. Duff*
Canada Centre for Remote Sensing, 2464 Sheffield Road,
Ottawa, Ontario K1A 0Y7, Canada

Anthony J. Fitzgerald
Roy Ball Associates, 1750 Courtwood Crescent,
Ottawa, Ontario K2C 2B5, Canada

ABSTRACT: The procedure defined by the Canada Centre for Remote Sensing (CCRS) for the radiometric correction of Landsat Thematic Mapper (TM) data from both Landsat-4 and Landsat-5 has been successfully implemented in a limited production environment. This production system, the CCRS TM Transcription System (TMTS), has geometric processing restricted to corrections for differences in line lengths and for Earth rotation effects, using nearest neighbor resampling. The film and digital products generated by the system are routinely distributed to Canadian users and have also been used for extensive testing of the radiometric calibration and correction procedure. The radiometric accuracy of these TM products is specified to be within 0.8 percent (2 digital levels) and is assessed in relation to three important aspects, namely, within-scene variability, overall differences between individual scenes recorded by the same sensor, and discrepancies between radiometric values within one scene recorded simultaneously by the two TM sensors.

INTRODUCTION

THE PROCEDURE CHOSEN by the Canada Centre for Remote Sensing (CCRS) for the radiometric calibration and correction of the reflective bands of Thematic Mapper (TM) data is based on the method used by CCRS for Landsat Multispectral Scanner (MSS) data, as reported by Ahern and Murphy (1978) and as refined by Murphy (1981). The method relies on combining the absolute calibration parameters of one reference detector in each band, as determined using the internal calibration system, together with the intraband relative correction parameters, as determined from the statistics of the raw data accumulated over a full Landsat scene, to yield the absolute calibration parameters for all detectors in all bands. Under the assumption that the response of all TM detectors is linear, the calibration parameters can be reduced to a set of unique scene-dependent gain and bias pairs, one pair for each mirror scan direction of each detector. A major difference between the TM and MSS radiometric correction methodologies stems from the fact that the TM zero-radiance reference level is nominally set to 3 digital counts (DN) and is updated before each sweep of the TM mirror. This is in contrast to the case of the MSS sensor, where the black-level output is neither directly measured nor altered on board the spacecraft after launch. Since the TM background reference level can be measured during the calibration period, an additional bias, which is a function of scanline number, is included in the TM radiometric correction parameters. Correction is also made for this line-dependent background level change when accumulating the scene statistics and when processing the internal calibration data, as described by Murphy *et al.* (1984). The application of the radiometric correction parameters can be represented by the following equation:

$$P_o(B,D,S,L,N) = \frac{1}{G(B,D,S)} *[P_i(B,D,S,L,N) - B_1(B,D,S) - B_2(B,D,S,L) - B_3(B,D,S,L,N)] \quad (1)$$

where:

P_o is output pixel value,
G is gain factor, which is constant for the scene,
P_i is input pixel value,

PHOTOGRAMMETRIC ENGINEERING AND REMOTE SENSING,
Vol. 51, No. 9, September 1985, pp. 1359-1369.

0099-1112/85/5109-1359$02.25/0

B_1 is bias factor, which is constant for the scene,
B_2 is bias factor, which is constant for the line,
B_3 is bias factor, which varies with pixel number,

and where:

B is the spectral band number,
D is the detector number within band,
S is the scan direction (forward or reverse),
L is the scanline number,
N is the pixel number within scanline.

Within-scene radiometric variability and residual striping can be described with reference to six identifiable TM sensor characteristics, and a summary of the identification and relative significance of each one is provided in the first section. It is shown that the CCRS correction procedure has the potential to reduce or eliminate three of these effects in the majority of TM scenes requested by users. However, extended bright targets located either at the western or eastern edges of a scene can affect background reference level measurements and hence degrade the striping removal. This effect is discussed in detail in the second section.

The third section discusses the accuracy of absolute calibration utilizing the in-flight calibration data by referring to simultaneous acquisitions of selected scenes from the concurrent overflight of Landsat-4 and Landsat-5 on 15 March 1984. This was accomplished by comparing the means and standard deviations derived from the histograms of identical ground target areas. In addition, using similar techniques, intercomparison was made between one scene fully processed by NASA/NOAA using the Thematic Mapper Image Processing System (TIPS) system and the identical scene, processed by CCRS using TMTS (Butlin and Murphy, 1983).

CHARACTERIZATION OF WITHIN-SCENE RADIOMETRIC VARIABILITY

A total of six major sources of systematic or slowly changing radiometric variability within any one band can be identified, and the method utilized by CCRS for the radiometric calibration and correction of TM data has the potential to reduce or eliminate three of these effects. These TM specific types of noise and residual striping can readily be displayed by simple contrast stretching. Since they could impact image classification, they are therefore discussed in relation to the radiometric quality of individual scenes. The terminology is the same as that used by Barker (1985).

Bin-Radiance Dependence

Bin-radiance dependence is a TM noise type associated with nonlinearities in the analog-to-digital (A/D) converters (Barker, 1985). Threshold voltages for some digital numbers (DN) (or bins) may be displaced by up to two DN, and there is a variation in bin width or voltage range per bin, as large as 2 DN. Bin-radiance dependence manifests itself as saw-toothed histograms of the raw data, as shown in Figure 1. The general shape of the saw-tooth is similar for all detectors within one band because the same A/D converter is used. There is also a similarity between bands, because a common design was used for all A/D converters. This type of error is not correctable in a deterministic sense although statistical corrections are possible.

Coherent Noise

Bands 1 to 4 of Landsat-4 exhibit coherent noise at two frequencies, namely 32.8 KHz and 5.9 KHz. Most detectors of Landsat-5 have coherent noise at only one frequency, 8.5 KHz, or multiples of it. These peak frequencies were established by Barker (1985), using Fourier analysis. Maximum amplitudes are less than 0.5 DN, except for a few detectors in band 1 of both Landsat-4 and Landsat-5. Since reduction of this type of noise could require the use of Fourier transforms, corrections are not performed.

Scan-Correlated Shifts

Observations of scenes of fairly uniform intensity such as large water bodies (for example, Murphy, 1984) have shown that the background reference level appears to be constant within a scanline, but can change from scanline to scanline by as much as 4 DN. (Although the nominal value for the background level is 3 DN, CCRS observations show the average value to be close to 2.5 DN.) This change in background level is referred to as a "scan-correlated shift." Moreover, the change has been observed to occur, not when the zero-radiance reference level was being reset, but rather at the start of each scanline. The magnitude of the shift from line to line depends on the particular detector, but if a shift is present for one detector, then a shift is present for all detectors for all bands. Figure 2 shows the relationship between the variation in image mean value and the background reference level for band 1 over a rectangular subscene of size 192 lines by 100 pixels extracted from a uniform test scene. (In this figure, the image mean values and the background DC values are plotted as deviations from the average value accumulated over the entire subscene.) Under the assumptions that the background level is constant within a line, and that this level can be determined from measurements during the calibration period, then the radiometric correction procedure described above accommodates scan-correlated shifts.

Within-Line Droop

Metzler and Malila (1985) and Malila *et al.* (1984) have characterized within-line droop by comparing

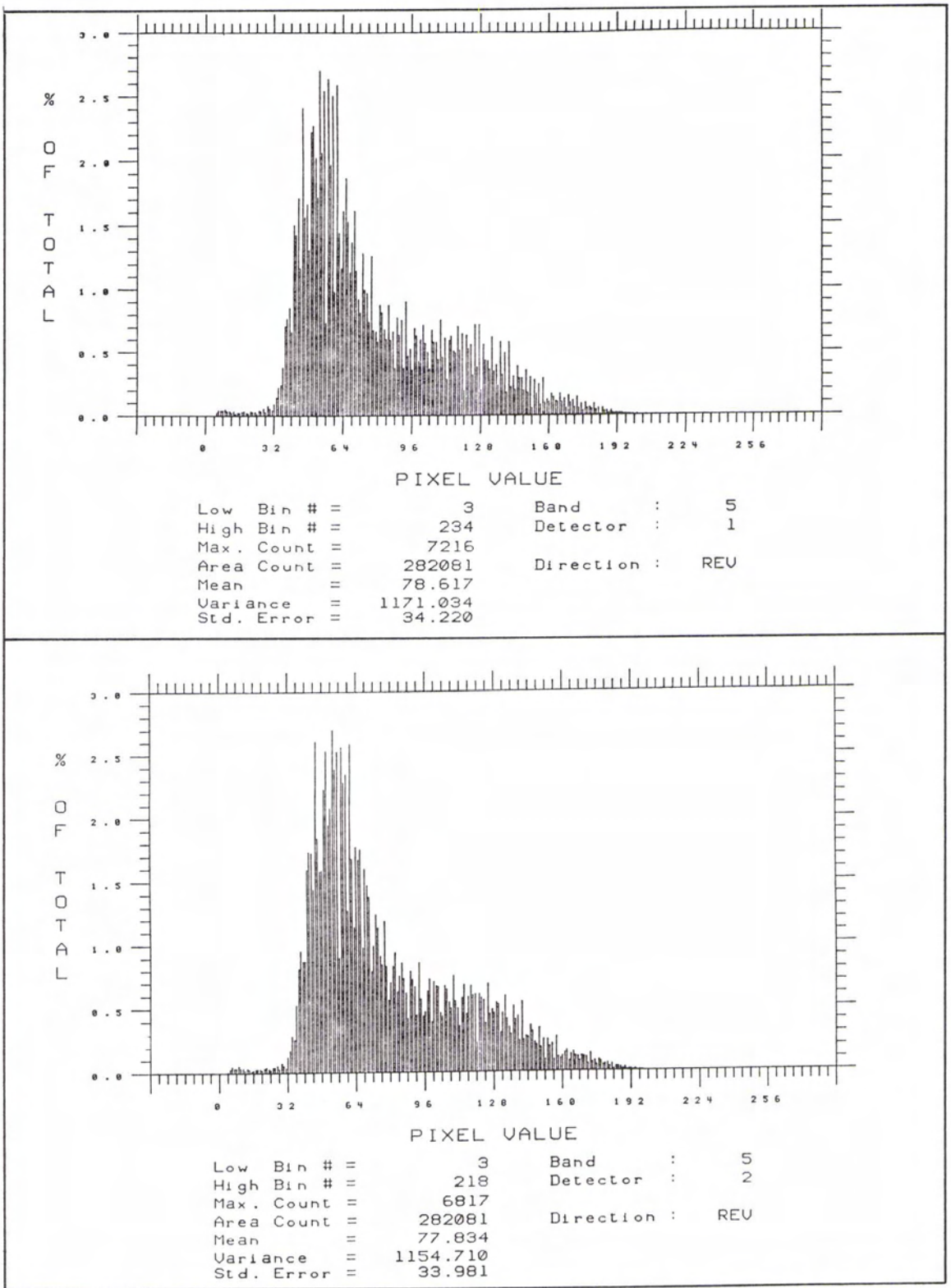

FIG. 1. Example of saw-toothed histograms caused by bin-radiance dependence, for two detectors of spectral band 5 of Landsat-5.

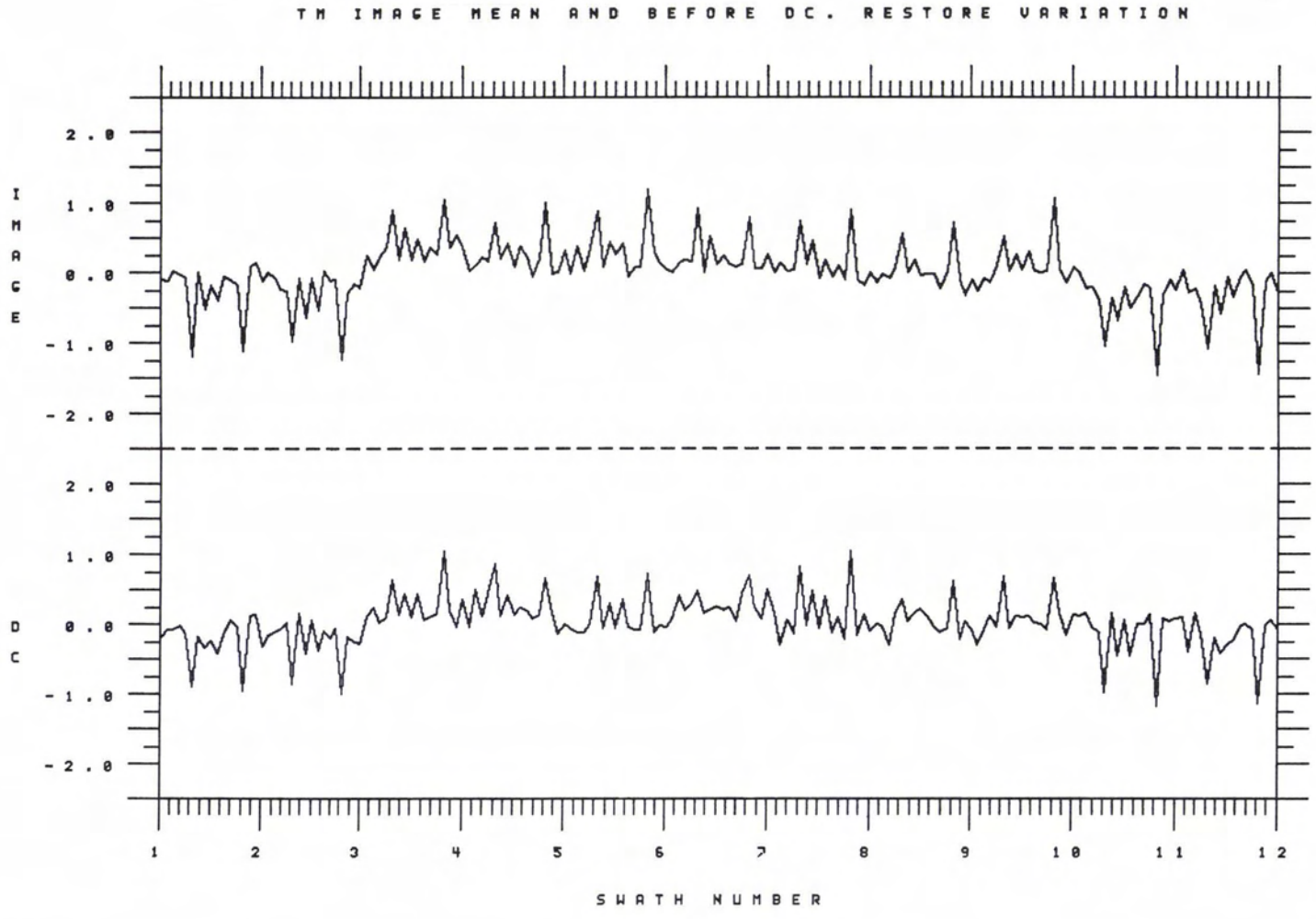

FIG. 2. Relationship between the variation in image mean value and the background reference level for band 1 of Landsat-4 over a rectangular subscene of size 192 lines by 100 pixels.

pixel values in the forward west-to-east scans with reverse east-to-west scans as a function of pixel number within the scene. The maximum observed effect was about 0.75 DN for band 1, between the maximum value at the start of the scan and the end of the active scan, with the droop being proportional to the magnitude of the signal. Pixel-dependent corrections are possible in the CCRS correction procedure and work is in progress to determine the mathematical model for the effect.

Forward-Reverse Scan Differences

Characterization of differences due to scan direction is hampered by the existence of the other five types of radiometric variability. However, absolute calibration data and scene statistics are treated by TMTS as though the forward and reverse scans were recorded by two separate sets of detectors. Any potential differences will therefore be automatically accommodated, with an insignificant overhead in processing time. (For scenes with no saturation, the differences between the forward and reverse gains and biases as deduced from scene statistics are of the order of 0.5 percent for the gains and less than 0.02 DN for the biases.)

Bright Target Effects

Immediately after exposure to an extended target such as snow, ice, or clouds, which is sufficiently bright to cause the detectors to reach the saturation region, the background reference level, and hence the recorded signal level, drop below nominal values. The signal level may be depressed by as much as 4 DN, taking up to 1000 pixels to return to its correct value, in an approximately exponential way. Hence after 500 pixels, the signal level is less than 2 DN away from its correct value. Forward mirror sweeps will therefore be darker after exposure (to the east) of these targets than they were before exposure (to the west). Conversely, reverse mirror sweeps will be darker to the west of these targets than they were before exposure (to the east). This gives the appearance of localized banding, in groups of 16 scanlines (corresponding to either a forward or reverse mirror sweep), extending for as much as 1000 pixels on both sides of the bright features. The effect on the scene as a whole is shown schematically in Figure 3. In scenes where these bright targets are located at least 1000 pixels away from both ends of the scanline, only those areas in the vicinity of the bright targets are affected. Figure 4 represents this case schematically, where the recorded and nominal signal levels are shown separately for forward and reverse scans. Figure 4 also indicates significant events during the scan period, with scene data being recorded between the start-of-line and end-of-line signals. Soon after the end-of-line signal, the shutter obscuration period (or exposure to a nominal zero-radiance reference level) occurs, and the detector is subsequently exposed to a calibration source (not shown). More significantly, this is also the period during which the zero-radiance reference level (DC) is updated. Hence, two measurements of DC values are available, one before DC restoration (BDC), and one after DC restoration (ADC). In the case shown in Figure 4, the bright target is sufficiently far away from the end-of-line on both forward and reverse sweeps for the background reference level to have recovered to its nominal value before shutter obscuration occurs. Subsequent use of the background reference levels in the calibration and correction procedure is unaffected by the bright target. Correction for localized bright target effects is not included in the CCRS correction procedure outlined in the introduction since an additional offset term as a function of the digital values of previous pixels would be required.

For scenes in which the bright target is located less than 1000 pixels away from either edge of the scene, background level measurements are also affected. Since this effect can degrade the quality of the image on a more global scale, it is discussed in more detail in the next section.

Characterization of Global Within-Scene Radiometric Variability

In addition to the localized light and dark banding effect described in the first section, extended bright targets are potentially a cause of three other forms of image degradation. Two of these are a direct result of including erroneous data in the full-scene histograms in generating relative (detector-to-detector) correction parameters. The third is due to the use of inappropriate background reference levels, where these have been artificially depressed by the bright target.

Detector Saturation

Different values of scene radiance cause saturation for individual detectors within a band. Hence the statistical distribution of scene radiances will not be similar for each detector, which could cause errors in the relative gains and offsets computed from the means and standard deviations. However, the refinements to the CCRS destriping procedure (Murphy, 1981) provide adequate compensation, and there is no induced image degradation.

Additional Forward-Reverse Scan Differences

In scenes where an extended bright target is located within 1000 pixels of the end of the active scan period, the background reference level during shutter obscuration remains below the value which it held before exposure to the bright source. This is shown schematically in Figure 5. The BDC value may be as much as 4 DN below the nominal value, the magnitude of the deviation being dependent both on the proximity of the bright target to the end

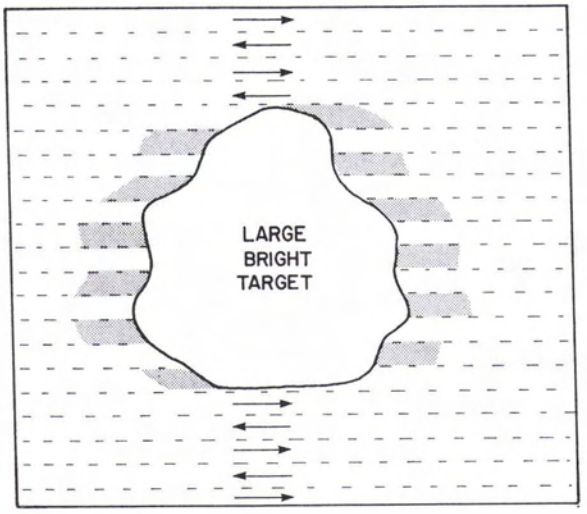

FIG. 3. Schematic representation of visual effect of bright target on signal levels.

of the scanline and on the nominal DC value for the scanline. In addition, since the DC restore function does not operate long enough to fully restore the background level to the value held at the beginning of the scanline, the ADC value is not representative for that line.

Hence, when correcting the forward (west-to-east) mirror sweeps, represented in Figure 5, for scan-correlated shifts, the DC value subtracted will be too low. However, for reverse (east-to-west) mirror sweeps, the DC value will be correct. The overall result is an additional small forward-reverse scan difference extending along the whole line, superimposed on the localized banding close to the target.

Full-Scene Bright Target Effects

When accumulating scene statistics, compensation for scan-correlated shifts is included and may be considered as a shift of the histogram for the line to a lower digital value. The use of BDC (or ADC) values which have been affected by bright targets will result in forward mirror sweeps (in the case represented in Figure 5) having mean values which are too high.

Therefore, the biases to be applied to all detectors for the full scene will be different for forward and reverse sweeps. Again, the magnitude of the effect depends on both the precise location and extent of the target and on the magnitude of the scan-correlated shifts.

ASSESSMENT OF ACCURACY OF ABSOLUTE CALIBRATION

Procedure for Comparison of Data Sets

The comparison of data sets, either acquired by different sensors or processed using different processing facilities, was simplified by utilizing a three-stage procedure. In the first stage (CCRS products only), TMTS was used for the application of intraband relative correction parameters and for adjustments for the bias $B_2(B,D,S,L)$ in Equation (1) to account for scan-correlated shifts. This was effected by setting the gain and scene-dependent bias ($G(B,D,S)$ and $B_1(B,D,S)$ respectively, in Equation 1) to 1 and 0, for each of the reference detectors. Manipulation of the raw data histograms was used to establish relative gains and scene-dependent biases for the other detectors, as explained in the Introduction. (The pixel-dependent correction $B_3(B,D,S,L,N)$ in Equation (1) was not used.) The TMTS products have therefore been corrected for detector-to-detector striping, scan-correlated shifts, and forward-reverse scan differences. This level of correction is referred to as *CAL1*, in a manner analogous to the terminology used by CCRS for Landsat MSS data (Ahern and Murphy, 1978). Data which have been calibrated to the radiance range recommended by NASA are referred to as *CAL2* data.

In the second stage, subscenes of data were selected from the scenes (after correction by TMTS, where appropriate), and the mean ($MEAN_{CAL1}$) and standard deviation ($STDEV_{CAL1}$) were deduced from histograms of the subscenes. For products generated on TMTS, the in-flight calibration data is processed separately, to yield the absolute calibration parameters, $G(B,D,S)$ and $B_1(B,D,S)$, for the reference detectors. The third and final stage consists of calculating the equivalent calibrated mean ($MEAN_{CAL2}$) and calibrated standard deviation ($STDEV_{CAL2}$) as follows:

$$MEAN_{CAL2} = (MEAN_{CAL1} - B_1(B,D,S))/G(B,D,S) \quad (2)$$

$$STDEV_{CAL2} = (STDEV_{CAL1})/G(B,D,S) \quad (3)$$

For data sets processed using the NASA/NOAA TIPS, no further absolute calibration is required.

Calculation of Absolute Calibration Parameters

Determination of the absolute calibration parameters for one reference detector in each band is performed by extracting and averaging the calibration pulses from within the raw data stream for each scanline in turn. An average digital number (DN) for each of the eight calibration states (after ignoring overshoot, warm-up time, and cool-down time) is then combined with the corresponding prelaunch radiance levels to yield the absolute gain and bias

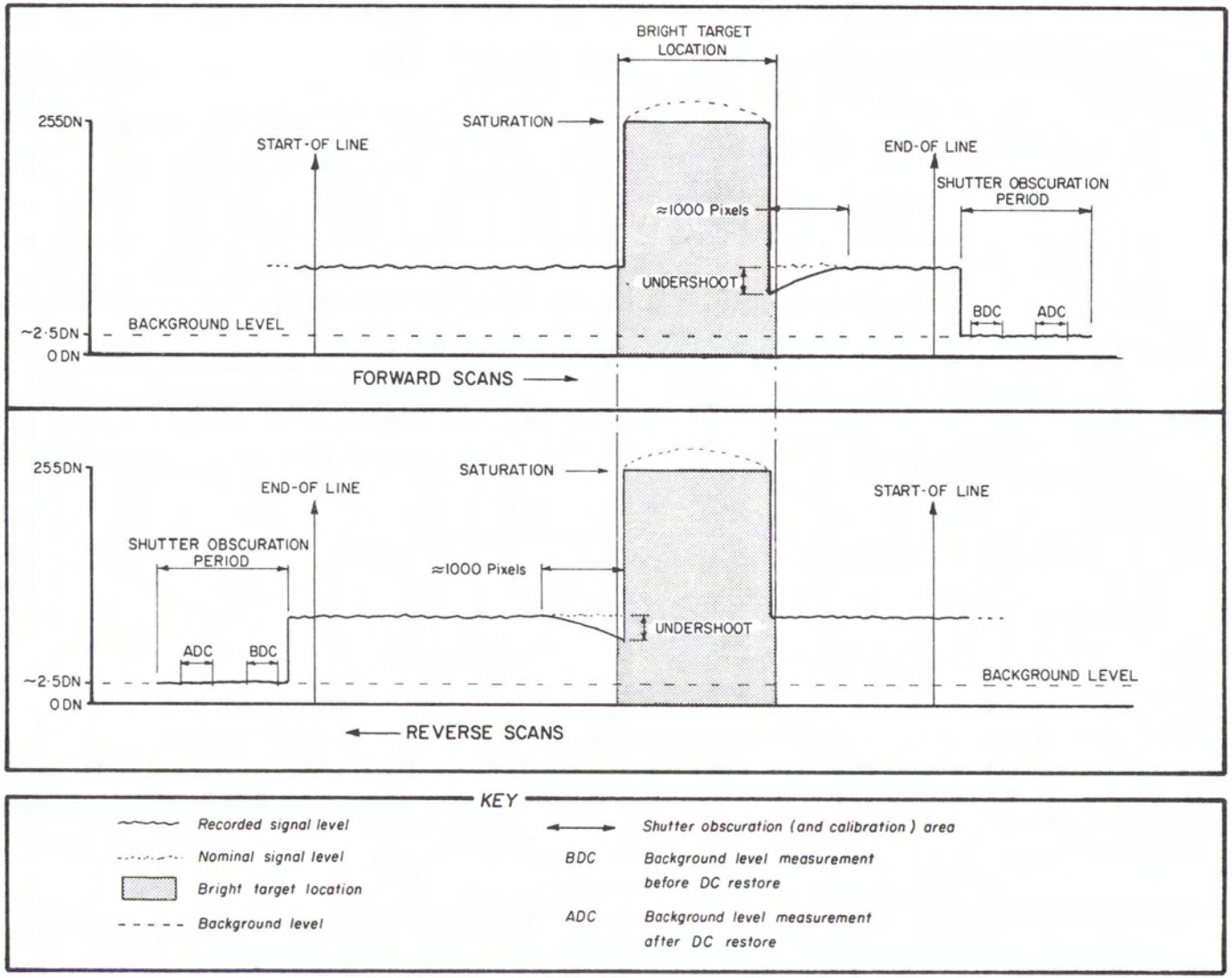

FIG. 4. Effect of bright target on signal levels recorded in forward (west-east) and reverse (east-west) mirror sweeps—Case 1. Bright target near center of scene.

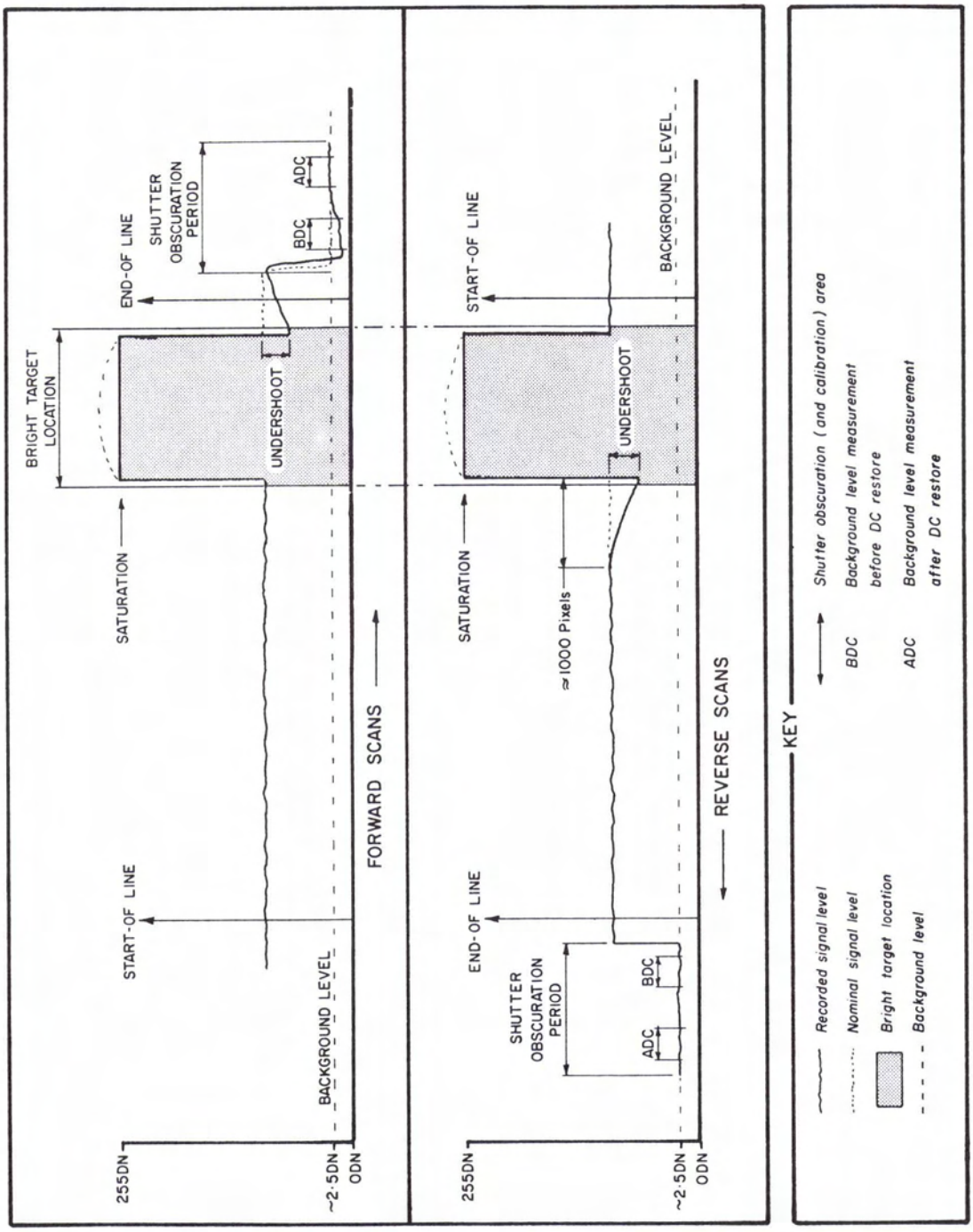

FIG. 5. Effect of bright target on signal levels recorded in forward (west-east) and reverse (east-west) mirror sweeps—Case 2. Bright target at edge of scene.

($G(B,D,S)$ and $B_I(B,D,S)$ respectively, in Equation 1) for each of the reference detectors. In order to minimize fluctuations due to scan-correlated shifts, the background reference level measurement immediately preceding the calibration pulse is subtracted from the calibration pulse average for each line, as explained by Murphy *et al.* (1984). (No correction for bright target recovery is required, since the calibration pulses are located very close to the locations for background level measurements.) The prelaunch radiance levels and radiance ranges for the individual bands used in the calculation of gains and biases are those recommended by Barker (1985) for Landsat-4, and also by Barker (unpublished data, 1984) for Landsat-5. In addition, since the recommended radiance ranges for Landsat-4 and Landsat-5 are identical, data sets from the two satellites can be compared using calibrated digital numbers without further processing to radiance units.

Selection of Subscene for Comparison of Data Processed by TMTS and by TIPS

One scene of data, identified as path 20, row 36, 50014-15454, acquired by Landsat-5 as part of the simultaneous overpass of Landsat-4 and Landsat-5 on 15 march 1984, was used in the comparison of data processed by TMTS and by the NOAA/NASA Thematic Mapper Image Processing System (TIPS). The TIPS data were processed on 28 June 1984 with full radiometric and geometric corrections, and resampled to a 28.5 m pixel size. Data corrected to this level are termed P-data (Irons, 1985). The TMTS data were processed on 29 November 1984 with a nominal 30 m pixel size (Butlin and Murphy, 1983). The subscene of data, of size 512 pixels by 512 lines in the TMTS products, encompassed Weiss Reservoir and started at line 577, pixel 1500 of quadrant 4. In order to enclose an identical ground area, the subscene of data from the TIPS product was of size 539 pixels by 539 lines and started at line 1155, pixel 2050 of quadrant 4. The calibration data used by TIPS are not corrected for scan-correlated shifts. To compare corresponding absolute values, it was necessary to use similarly uncorrected calibration pulse values in the calculation of absolute calibration parameters to be applied to the TMTS data set in the third stage.

Selection of Subscenes for Comparison of Data Acquired by Landsat-4 and Landsat-5

Two scenes of data, acquired simultaneously on 15 March 1984, were used in the comparison of the absolute calibration of the Landsat-4 and Landsat-5 TM sensors, namely, path 20, row 36 and path 20, row 16. The Landsat-4 TMTS scene, identified as path 20, row 36, 40608-15461 was processed on 17 February 1985. The equivalent ground area started at line 577, pixel 1100 of quadrant 4. The Landsat-5 TMTS scene was the same one used in the TMTS/TIPS comparison.

The second pair of scenes, identified as path 20, row 16, 50014-15373 from Landsat-5 processed on 7 December 1984, and as path 20, row 16, 40608-15380 from Landsat-4 processed on 6 December 1984 were also compared in order to include a larger dynamic range in the test data. The selected subscene started at line 1130, pixel 2480 for Landsat-4 and line 2100, pixel 2500 for Landsat-5. For both pairs of scenes, the calibration pulse values for both Landsat-4 and Landsat-5 used in generating absolute calibration parameters were corrected for scan-correlated shifts.

Results of Comparisons

The calibrated means and calibrated sigmas for the Landsat-5 TIPS and TMTS data sets are shown in Table 1.1 for an overview of the whole subscene, and in Table 1.2 for a smaller water target. The difference between the TMTS and TIPS values is in the range of 2 to 5 digital numbers (DN) for all bands. However, observation of the raw digital values for the water target, yielding mean values of 5.3 DN and 3.4 DN for bands 5 and 7 respectively, indicates that the calibrated TIPS values (1.7 DN and 0 DN for bands 5 and 7 respectively) have been forced off-

Table 1. Comparison of TMTS/TIPS Calibrated Data Sets

Table 1.1 Landsat-5 TM TIPS vs. TMTS—Overview

Band	Landsat-5 TIPS Mean	Landsat-5 TIPS Sigma	Landsat-5 TMTS Mean	Landsat-5 TMTS Sigma	(TMTS − TIPS) Mean
1	86.8	7.3	90.0	7.1	+3.2
2	36.4	6.0	39.0	5.8	+2.6
3	36.2	10.2	41.0	10.3	+4.8
4	37.8	21.5	39.4	20.2	+1.6
5	64.0	47.8	63.1	43.4	−0.9
7	23.5	21.9	31.1	21.9	+7.6

Table 1.2 Landsat-5 TM TIPS vs. TMTS—Water Only

1	86.7	1.4	89.9	1.6	+3.2
2	37.5	0.8	39.9	0.8	+2.4
3	30.7	0.9	35.7	1.0	+5.0
4	8.6	0.7	12.2	0.5	+3.6
5	1.7	0.9	6.5	1.3	+4.8*
7	0.0	0.1	5.0	0.8	+5.0*

* The mean and sigma for the completely raw downlinked data for bands 5 and 7 were:
Band 5 Mean = 5.3; SIGMA = 1.0
Band 7 Mean = 3.4; SIGMA = 1.1
This implies that the TIPS calibration has forced the data off-scale.

TABLE 2. COMPARISON OF LANDSAT-5 VS. LANDSAT-4 (ROW 36)

Table 2.1 Landsat-5 vs. Landsat-4 TMTS—Overview

	Landsat-5 TMTS		Landsat-4 TMTS		(Landsat-5 − Landsat-4)	
Band	Mean	Sigma	Mean	Sigma	Mean	% Difference
1	89.5	7.1	90.3	7.2	−0.8	[<1 DN]
2	38.0	5.8	34.3	5.1	+3.7	+10.8
3	40.0	10.3	39.9	9.8	+0.1	[<1 DN]
4	38.4	20.2	41.5	20.7	−3.1	−7.5
5	62.4	43.5	63.9	43.4	−1.5	[1 DN]
7	30.3	21.9	29.8	21.0	+0.5	[<1 DN]

Table 2.2 Landsat-5 vs. Landsat-4 TMTS—Water Only

1	89.4	1.6	90.2	1.8	−0.8	[<1 DN]
2	38.8	0.8	35.1	0.7	+3.7	+10.5
3	34.7	1.0	34.8	1.0	−0.1	[<1 DN]
4	11.2	0.5	13.2	0.5	−2.0	−15.1
5	5.7	1.3	6.4	4.1	−0.7	[<1 DN]
7	4.1	0.8	4.1	1.2	+0.0	[<1 DN]

scale. TMTS values are consistently higher than TIPS values.

The calibrated means and calibrated sigmas for the Landsat-5 and Landsat-4 TMTS data sets are shown in Table 2.1 (row 36) and Table 3.1 (row 16) for an overview of the whole subscene, and in Table 2.2 (row 36) and Table 3.2 (row 16) for a smaller water target. For bands 1, 5, and 7 there is very good agreement between the calibrated values for Landsat-4 and Landsat-5, the differences being less than 1.8 DN. For band 3, the Landsat-5 values are about 2 percent higher than Landsat-4 values. However, for band 4, Landsat-5 values are consistently lower than Landsat-4 values. An approximate relationship Landsat-5 = 0.96 * Landsat-4 − 2.0 was deduced by plotting the Landsat-5 values versus the Landsat-4 values and drawing a straight line to connect the points. For band 2, Landsat-5 values are consistently higher than Landsat-4 values, with an approximate relationship Landsat-5 = 1.12 * Landsat-4, deduced by a similar graphical approach.

SUMMARY

CCRS has utilized the Thematic Mapper Transcription System to generate raw data products to be used in the analysis of the radiometric characteristics of Landsat-4 and Landsat-5 Thematic Mapper data. In addition, raw calibration data have been used in the development of the algorithms to process the in-flight calibration data. As a result of these studies, the radiometric correction algorithms to be used in generating TMTS products have been refined to include radiometric corrections for scan-correlated shifts, forward/reverse mirror scan differences, and for factors which may vary as a simple function of increasing pixel number within a scanline. Assessment of intraband relative radiometric errors of approximately 100 scenes corrected on TMTS shows the accuracy to be well within the 0.8 percent RMS-of-full-scale (2 DN) specified for Canadian ground processing systems for the majority of scenes. However, for scenes containing extended bright targets, residual radiometric banding exceeds specifications for about 500 pixels on either side of the target. In addition, for scenes containing extended bright targets that are located at either the eastern or western extremity, residual radiometric banding exceeds specifications for the full extent of scanlines containing these targets. Investigations are continuing to further quantify and compensate for these effects.

TABLE 3. COMPARISON OF LANDSAT-5 VS. LANDSAT-4 (ROW 16)

Table 3.1 Landsat-5 vs. Landsat-4 TMTS—Overview

	Landsat-5 TMTS		Landsat-4 TMTS		(Landsat-5 − Landsat-4)	
Band	Mean	Sigma	Mean	Sigma	Mean	% Difference
1	[Off-scale]		[Off-scale]		[ ]	[ ]
2	116.4	35.3	103.6	26.5	+12.8	+12.4
3	140.1	39.1	137.4	40.0	+2.7	+2.0
4	96.2	33.7	101.7	35.1	−5.5	−5.4
5	42.8	17.6	41.5	16.8	+1.3	[1 DN]
7	24.5	10.2	24.5	10.4	+0.0	[<1 DN]

Table 3.2 Landsat-5 vs. Landsat-4—Water Only

1	120.5	5.3	118.7	3.2	+1.8	+1.5
2	40.1	2.4	35.7	1.7	+4.4	+12.3
3	39.6	3.1	38.6	2.5	+1.0	[<1 DN]
4	20.0	1.4	23.4	1.8	−3.4	−14.5
5	7.3	1.7	7.8	1.3	−0.5	[<1 DN]
7	5.5	1.3	5.4	1.0	+0.1	[<1 DN]

Comparison of one scene processed on the NASA/NOAA TIPS system and on the CCRS TMTS system shows that the TMTS values range from 1 to 5 DN higher than TIPS values. Comparison of two scenes recorded simultaneously by the Landsat-5 and Landsat-4 TM sensors shows the absolute calibration for bands 1, 3, 5, and 7 to be in excellent agreement. However, for band 4, Landsat-5 values are consistently lower than Landsat-4 values, and for band 2, Landsat-5 values are more than 10 percent higher than Landsat-4 values.

Based on the encouraging results from these studies, the intraband relative correction algorithms and the absolute calibration algorithms will be implemented in the MOSAICS production system (Guertin *et al.*, 1984) that will replace TMTS in 1986.

REFERENCES

Ahern, F. J., and Murphy, J., 1978. Radiometric Calibration and Correction of LANDSAT 1, 2 and 3 MSS Data: Canada Centre for Remote Sensing, Research Report 78-4.

Barker, J., 1983. Relative Radiometric Calibration of TM Reflective Bands: *Landsat-4 Science Characterization Early Results*, NASA Conference Publication 2355, Vol. III, pp. III-1 to III-219.

Butlin, T., and Murphy, J., 1983. Early Processing of Thematic Mapper Data by the Canada Centre for Remote Sensing: *Proceedings 17th International Symposium on Remote Sensing of Environment*, pp. 1383-1392.

Guertin, F. E., Friedmann, D., Simard, R., Brown, R. J., and Teillet, P. M., 1984. Multiple Sensor Geocoded Data: *Proceedings of Committee on Space Research 1984*, Graz, Austria.

Irons, J. R., 1983. An Overview of LANDSAT-4 and the Thematic Mapper: *Landsat-4 Science Characterization Early Results*, NASA Conference Publication 2355, Vol. II, pp. II-15 to II-46.

Malila, W. A., Metzler, M. D., Rice, D. P., and Crist, E. P., 1984. Characterization of LANDSAT-4 MSS and TM Digital Image Data: *IEEE Transactions on Geoscience and Remote Sensing*, v. GE-22, no. 3 (May), pp. 171-191.

Metzler, M. D., and Malila, W. A., 1985. Characterization and Comparison of Landsat-4 and Landsat-5 Thematic Mapper Data: *Photogrammetric Engineering and Remote Sensing*, (this issue).

Murphy, J. M., 1981. Refined Destriping Procedure for LANDSAT MSS Data Products: *Proceedings 7th Canadian Symposium on Remote Sensing*, pp. 454-470.

Murphy, J. M., Butlin, T., Duff, P. F., and Fitzgerald, A. J., 1984. Revised Radiometric Calibration Technique for LANDSAT-4 Thematic Mapper Data: *IEEE Transactions on Geoscience and Remote Sensing*, v. GE-22, no. 3 (May), pp. 243-251.
